

Numerical Investigation of the Effects of Different Basin Materials of Single Slope Solar Water Still Using Computational Fluid Dynamics

¹Umar S., ¹Uthman M. I., ¹Gado A.A and ¹Shehu M

¹Department of Physics, Kebbi University of Science and Technology, Aliero Kebbi, Nigeria.

Date of Submission: 01-03-2025

Date of Acceptance: 10-03-2025

ABSTRACT

The scarcity of clean drinking water remains a pressing global challenge, necessitating sustainable and efficient water desalination solutions. This study investigates the performance of single-slope solar water distillers using different basin materials {Copper (Cu), Aluminum (Al), and Galvanized Iron (GI)} through Computational Fluid Dynamics (CFD) simulations conducted via ANSYS FLUENT. The thermal properties of these materials significantly influenced distillation efficiency and water yield. Results indicate that distillers with copper basins achieved the highest daily distillate yield of 2.73 L/day and efficiency of 61.85%, followed by aluminum (2.61 L/day, 59.13%) then galvanized iron (2.56 L/day, 57.99%). Copper's superior thermal conductivity and lower water depth facilitated faster heating and evaporation, enhancing performance. These study shows the potential of optimizing basin material selection to improve solar still productivity, making it a viable solution for water-scarce regions.

KEYWORDS: Solar distillation, basin materials, ANSYS FLUENT, Computational Fluid Dynamics (CFD) and renewable energy.

I. INTRODUCTION

Water is known to be the most essential and basic need for human beings, along with food and air required for sustaining life on Earth (Mishra, 2023). Water and the life of human beings are interrelated to each other (Muntean et al., 2021). Water is considered to play one of the pivotal roles in the development and welfare of any civilization. Every field associated with human life is directly or indirectly dependent on clean drinking water (Appiah et al., 2023). Due to this reason, the availability of pure and clean drinking water is

considered one of the major global issues as per the current scenario of the world (Mukhopadhyay et al., 2022).

Water is the most unique and invaluable gift to living beings from nature that is abundantly present on Earth (Ashokkumaret al., 2022). Out of the total available water on Earth, 97% is in the ocean in the form of saline water, approximately 2% of water is covered by ice in polar regions, and only the remaining one percent can be used to fulfill the needs of plants, animals and human life that is available in the forms of lakes, rivers and underground water (Appiah et al., 2023). Though this small share of accessible clean water is sufficient to lead to human life and other usage, rapid population growth and fast industrialization is narrowing the access to potable water (Mishra et al., 2021).

Access to potable water is a growing concern as population growth and industrialization strain freshwater resources (Tariq et al., 2023). Traditional desalination methods such as reverse osmosis and multi-stage distillation, while effective, are energy-intensive and costly, limiting their application in rural and remote areas (Elewa et al., 2024).

The demand for economical freshwater production has resulted in the research and development of various water desalination techniques (Ahmed et al., 2021). These water desalination techniques must be economical, simple to build, pollution free and efficient in energy to be feasible for remote areas (Alawad et al., 2023). The single slope solar still meets all these requirements for becoming a sustainable method of water desalination (Chauhan et al., 2021). Solar still uses solar energy, which is renewable energy, for its operation, due to which no electricity is required

for its operation (Makaet al., 2022). It is also environment friendly and its design is very simple such that anyone with minimum skills can also design it (Zallioet al., 2022). Furthermore, solar still could be made from locally available material. The major cost is only the fabrication cost.

Solar water distillation provides a sustainable alternative, utilizing solar energy to evaporate and condense water, leaving impurities behind (Khashehchiet al., 2024). A single-slope solar still is one of the simplest and most economical designs, with its efficiency significantly influenced by the thermal properties of its basin material (Dubeyet al., 2022). Although solar stills have advantages of being economical, simple-design, environmental friendly and uses abundant solar energy for its operation, it has one disadvantage of being less productive in the distillate yields. This problem of low distillate yield, to a great extent could be improved by knowing various parameters of solar still and optimized it, in order to optimize the performance parameters, the modeling of solar still using ANSYS CFD analysis could be done.

Advancements in Computational Modeling, such as CFD tools like ANSYS FLUENT, enable researchers to simulate heat and mass transfer processes within solar stills (Kumaret al., 2024). This study intends to numerically simulate single slope solar water distiller with three different basin materials {Galvanized Iron (GI), Aluminum (Al) and Copper (Cu)} using CFD to evaluate the effects of different basin materials on the performance of a single-slope solar water still.

II. ENERGY EFFICIENCY

The overall thermal efficiency of the solar still is the ratio of evaporative heat transfer to the solar irradiance. Which can be expressed as:

$$\eta_{th} = \frac{\sum m \times L_w}{\sum I \times A \times t} \quad (1)$$

where m , L_w , A and t are daily sum of mass condensate collected, latent heat of vaporization of water, daily mean solar radiation, glass cover area and time for the collection respectively. This is similar to the equation adopted by (Jatharet al., 2022).

III. GOVERNING EQUATIONS

The below equations shows the steady-state condition model based on the equation of continuity, momentum, conservation of energy, and mass transfer laws. The incident solar radiation in the basin water is responsible for the heat transfer mechanism (Siva Sankaranet al., 2022).

i. Energy equation

The energy equation of the mixture,

$$\frac{\partial}{\partial t} \sum_{k=1}^n [\alpha_k \rho_k E_k + \nabla \cdot \sum_{k=1}^n (\alpha_k \bar{v}_k (\rho_k \rho E_k + p))] + [\alpha_k \bar{v}_k (\rho_k \rho E_k + p)] = \nabla \cdot (k_{eff} \nabla T) + S_E \quad (2)$$

Where, k_{eff} is effective conductivity $[\sum_{k=1}^n \alpha_k (k_k + k_t)]$, k_t is the thermal conductivity (W/mK), T is the temperature (K), S_E is the heat sources e.g., solar radiation absorbed by the basin. This is similar to the equation adopted by (Khashehchiet al., 2024).

ii. Continuity equation

The continuity equation of the mixture,

$$\frac{\partial}{\partial t} (\rho_m) + \nabla \cdot (\rho_m \bar{v}_m) = 0 \quad (3)$$

Where, \bar{v}_m is the average velocity of mass: $\bar{v}_m =$

$$\frac{\sum_{k=1}^n \alpha_k \rho_k \bar{v}_k}{\rho_m} \text{ and } p \text{ is the pressure (Pa).} \quad (4)$$

iii. Momentum equation

The momentum equation of the mixture can be acquired by adding each momentum equations for all the phases and it can be expressed as.

$$\frac{\partial}{\partial t} (\rho_m \bar{v}_m) + \nabla \cdot (\rho_m \bar{v}_m \bar{v}_m) = -\nabla p + \nabla \cdot [\mu_m (\nabla \bar{v}_m + \nabla \bar{v}_m^T)] + \rho_m \bar{g} + \bar{F} + \nabla \cdot (\sum (\alpha_k \rho_k \bar{v}_k d_{r,k} \bar{v}_k)) \quad (5)$$

Where, ρ is the pressure (Pa), μ is the dynamic viscosity (Pas) and \bar{F} is the body forces e.g., gravity. This is similar to the equation used by (Almajaliet al., 2024).

IV. TEMPERATURES AND PRODUCTIVITY

The hourly productivity of the solar still can be calculated as follows (Sonawaneet al., 2022).

$$m_w = \frac{L_{Ewgi} \times (T_w - T_{gi}) \times A}{L_{ev}} \quad (12)$$

The daily productivity of the still can be obtained as follows;

$$M_w = \sum_{i=1}^{24} m_w \quad (13)$$

Where, T_w is the basinwater temperature ($^{\circ}\text{C}$), T_{gi} is the glasscover temperature ($^{\circ}\text{C}$), L_{ev} is the latent heat of vaporization (JKg), L_{Ewgi} is the convective heat transfer coefficient for natural convection (from water to inner surface of the glass) ($\text{W}/\text{m}^2 \cdot \text{K}$) and A is the basin area (m^2). This is similar to the equation adopted by (Kumaret al., 2024).

V. METHODOLOGY

The three-dimensional geometry of single slope solar water distiller was modeled using ANSYS “Design Modeler” with all the geometrical constraints in the ANSYS workbench. The physical model of the solar still was then meshed using 3-D hexahedral meshing.

i. Geometric Model

The 2-D model was first sketch in the ANSYS WORKBENCH with the help of “DESIGN MODELER” by clicking on YZ-plane, the profile of single slope solar still together with the dimension $1.2\text{m} \times 0.35\text{m}$ and height of 0.16m . Clicking on “file” icon, extrude sketch 1 and apply within geometry. Then rotate to 3-D and extrude. Water depth was also set in the geometry as (5mm).



Plate1: Shows 3-D geometry of single slope solar distiller

ii. Meshing of the Solar Still

In the present research, considering the current geometry in plate 1 of single slope solar distiller as there is absence of any curved or complex surface, the type of the meshing chosen was Hexahedral meshing on the basis of literature reviews. Hexahedral meshing was also chosen because of the simpler rectangular geometry of solar stills in the current problem. This would result in accurate solutions in limited period of solver time (Kumaret al., 2024).

The element size used was 0.02m and maximum face size in the quality was also taken as 0.02m. Smoothing was kept as high. Element order is taken as linear. Relevance was set to 100 and relevance center as fine. After the generation of mesh, total number of nodes is 123240 and the total number of element present in the generated mesh is 114345 that is sufficient enough with respect to the current problem of solar stills. We then assign names to all boundaries e.g. Glass plate, absorber plate, adiabatic walls (front, side and back walls), update and closed meshing.

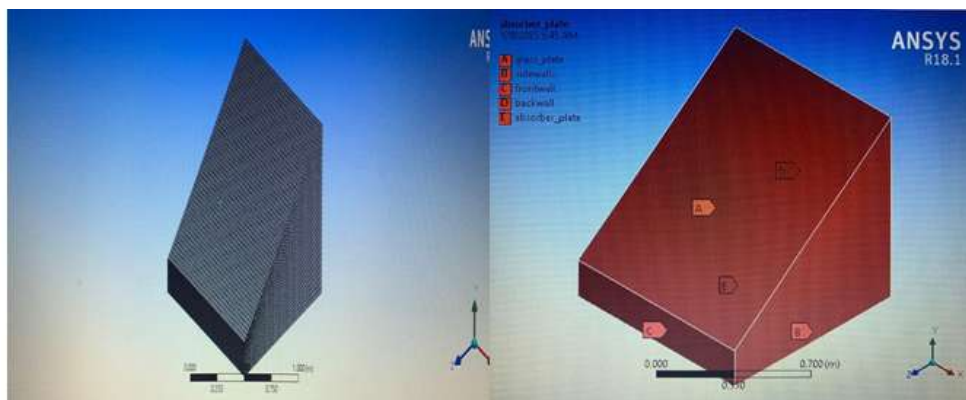


Plate2: Shows meshing model and naming of single slope solar distiller in ANSYS

Multi-phase VOF (volume of fluid) model with three phases, namely air, water-liquid and water-vapor are defined to model the evaporation-condensation process. Turbulence model used was RNG (renormalization group) k-epsilon with standard wall function. Side walls are insulated; hence, adiabatic wall conditions are applied. Adhesion forces are considered during analysis for producing water droplets on the inner wall surface of condensing glass. Air and water volume fractions are specified as 0.75 and 0.25 respectively. Operating pressure and temperature are taken as 1.01 bar and 403K respectively, with gravity in the negative Y direction. First-order upwind method is used for the momentum, energy, volume fraction, kinetic energy and dissipation rate as it gives a stable solution with a good rate of residual convergence. The convergence criterion for energy equation is set to 10^{-6} whereas for all other variables such as X, Y and Z velocity, continuity, energy, turbulent kinetic energy (k) and kinetic energy dissipation rate (ϵ), convergence criteria are taken as 10^{-3} .

iii. Specifying Materials

It is one of the very important parameters for simulation. Materials selection plays an important role in simulation (Sharma et al., 2022). Solids and fluids was involved in the current research. In fluids, there are air, water and vapor chosen as material from FLUENT Database for inner volume. In solid, the material of side walls are chosen as wood, basin was Galvanized Iron (GI) sheet, Aluminum (Al) and Copper (Cu) and the top of inclined cover was chosen as Glass. The data for Galvanized Iron (GI) sheet, Aluminum (Al), Copper (Cu) and Glass was chosen manually whereas data for other material was specified from FLUENT database. Then we define the mixture phases and phases interaction; air-primary phase, vapor-secondary phase and water-secondary phase. We then insert surface tension coefficient (n/m) as 0.073.

The properties of GI sheet, Aluminum, Copper and Glass was specified manually as follows:

Table 3.1: Materials Properties

Selected Materials	GI Sheet	Aluminum	Copper	Glass
Density (kg/m^3)	2235	2719	8978	2500
Sp. Heat Capacity (J/kg-K)	502	871	381	750
Thermal Conductivity (W/m-K)	55	202.4	387.6	1.15

iv. Specifying Boundary Conditions

Boundary condition plays an important role in simulation of any problem domain. The accuracy of the result and authentication of the result depends upon the correct specification of the boundary layer (Klewicki et al., 2024). Most condition are chosen as per practical applications

whereas some are chosen by the inbuilt algorithm of simulation software.

Initially, all the components was named as its components for the ease of the problem. Named selection was chosen during naming of the components. The brief of the boundary condition of solar still components are as follows;

Table 3.2: Boundary Conditions

Name and Type of Zone	Description	Wall Thickness (m)
Glass Top (Wall)	Radiation	0.015
Adiabatic Walls (All the sidewalls)	Adiabatic Wall (Heat flux = 0)	0.007
Basin Absorber (Wall)	Adiabatic Wall (Heat flux = 0)	0.007

v. Solution Initialization

In the present research, implicit type solver has been taken into consideration because it uses memory efficiently and the solved equations need to be stored once (Uncuoglu et al., 2022). First order takes less computational time whereas second order takes more time for computation of the

solution (Kumaret al., 2022). On the basis of time taken for calculation, the current research employed the use of first order upwind solution method.

Initially, the residuals of the X, Y and Z were observed till it reaches the convergence. The value for energy equation is kept 10^{-6} and it is kept

10-3 for all other variables. While defining the converging criteria, it is assumed that the obtained result will no longer diverges once the convergence has been achieved with more iterations (Sharma et al., 2022).

After all the parameters and variables have been specified, initialization of the solution was done. Number of iterations was chosen as 500, Time Step Size (s) was chosen as 30 and Number of Time Steps as 120 (Zadeet et al., 2023).

VI. RESULT AND DISCUSSIONS

ANSYS FLUENT was used to simulate the CFD technique. An unsteady simulation has been processed on 6th September, 2024 for 12hrs. From 0700hrs to 1800hrs in Aliero, Kebbi State, Nigeria. Located at latitude $12^{\circ} 17' 18''$ N and longitude $4^{\circ} 28' 17''$ E. For a solar still, temperature acquired in a glass cover, basin water, and inside a

chamber of the still, it plays a primary role in the water distillation process. Various contours such as static temperature, total temperature, and volume fraction of different phases processed at known intervals of time. The temperature contours of solar still are plotted periodically. It is observed that the temperature increases up to 1500hrs and then decreases gradually. This is due to increases in solar intensity up to 1500hrs after it decreases monotonically. The interior contours of water temperature also plotted with a specific time. It is observed that the water temperature begins to increase as solar radiation penetrates water through the glass cover. After a certain time, water begins heating and tends to evaporation. The interior contour temperature exposes the increment in the interior temperature of still with time concerning.

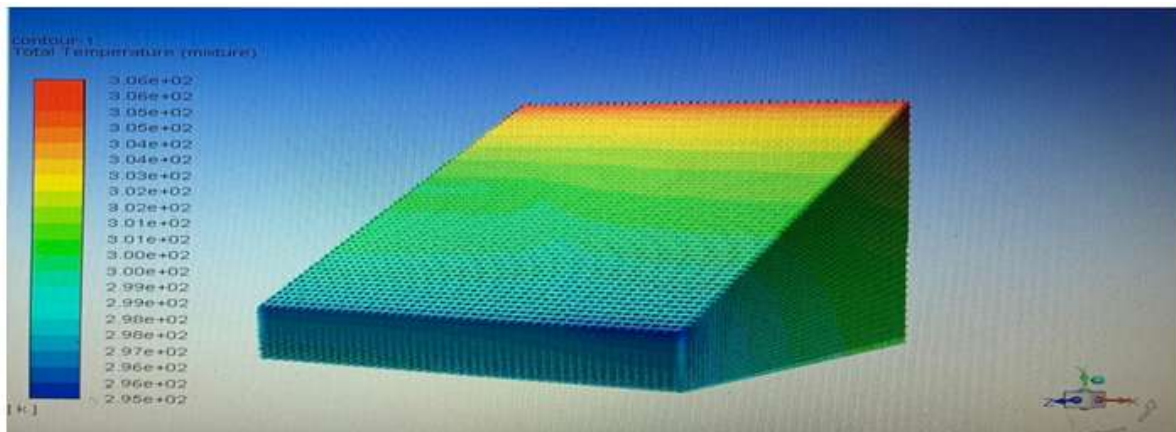


Plate3: Shows the total temperature contour

The variation of hourly distillate of solar stills made with basin materials of Galvanized Iron (GI), Aluminum (Al), and Copper (Cu) at (5mm) water depth is depicted in figure 4.1. It is clear from the graph that the yields were first recorded at 0900hrs given out 0.17 L/hr for Copper basin material, 0.15 L/hr for Aluminum basin material and 0.14 L/hr for Galvanized Iron basin material. The yields as seen from the figure increase as time of the day increases until it reaches peak at 1400hrs exactly when the solar radiation is high ($870\text{W}/\text{m}^2$), it then starts decreasing coming down till 1800hrs when the yields were recorded as 0.25 L/hr for Galvanized Iron basin material, 0.19 L/hr for

Copper basin material and 0.20 L/hr for Aluminum basin material. It shows clearly that still with Copper as basin material has the least yield followed by Aluminum then Galvanized Iron with the highest yield. This shows that the amount of distillates collected per hour is affected by design parameter either in the basin material or water depth (Ahmed et al., 2021). This also indicates that Copper (Cu) basin material at depth (5mm) achieved the highest cumulative daily yield followed by Aluminum (Al) then Galvanized Iron (GI). This is due to its higher thermal conductivity and lower or thinner water depth results in faster heating and evaporation (Almajali et al., 2024).

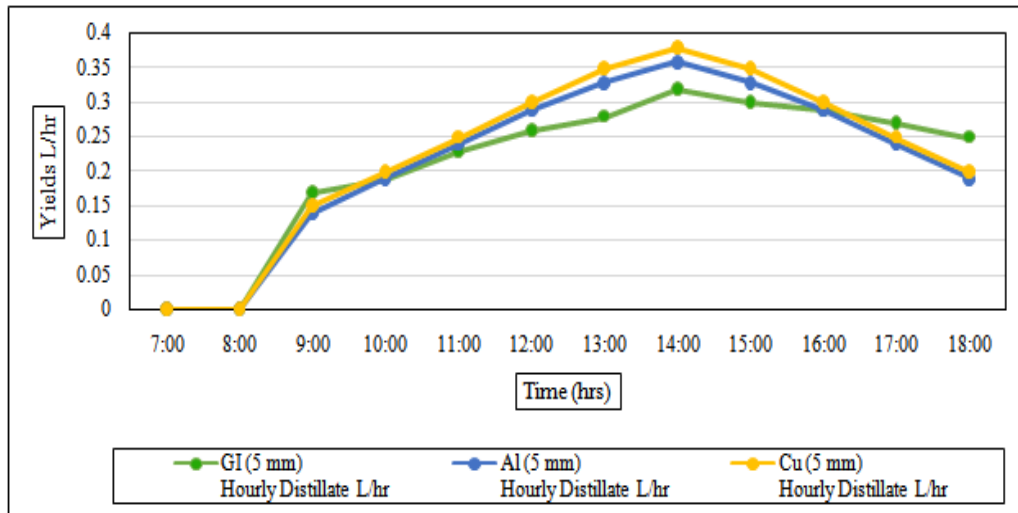


Figure 4.1: Variation of Hourly Distillate Yields at (5 mm) Water Depth with Time.

The difference between basin water temperature with glass cover temperature ($T_w - T_g$) at (5mm) water depth for different basin material still made with Galvanized Iron (GI), Aluminum (Al) and Copper (Cu) is depicted in figure 4.2. The graph above shows the same trend of distillate yields starting from 0900hrs reaching peak yields at 1400hrs and gradually decreasing until 1800hrs simultaneously. These temperature difference define the performance of solar still, the highest

temperature difference ($T_w - T_g$) for stills with basin Copper (Cu), Aluminum (Al) and Galvanized Iron (GI) at (5mm) water depth are 23°C, 21°C, 18°C respectively. It can be observed that the still with Copper (Cu) as basin material recorded highest temperature difference compared to stills with Galvanized Iron (GI) and Aluminum (Al). This is due to its higher thermal conductivity as compared to Galvanized Iron (GI) and Aluminum (Al) (Almajaliet al., 2024).

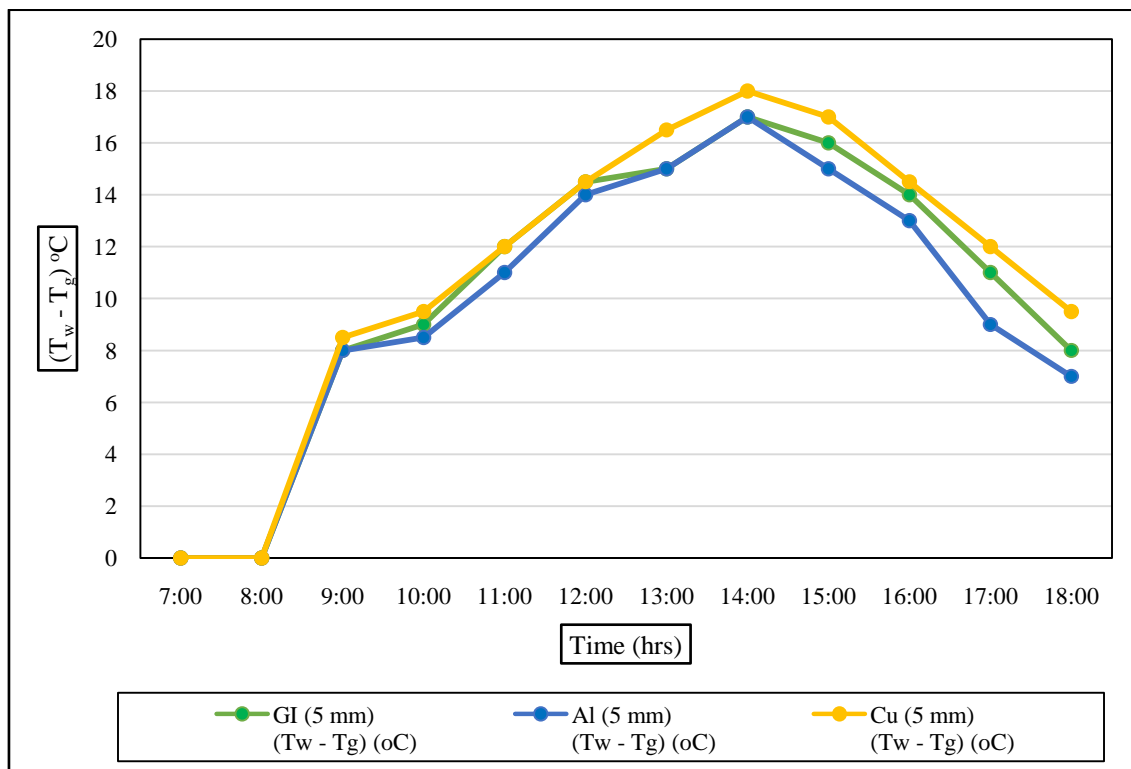


Figure 4.2: Plot of ($T_w - T_g$) °C with Local Time of the Day at (5mm) Water Depth.

The hourly variation of basinwater temperatures for stills made with different basin materials of Galvanized Iron (GI), Aluminum (Al) and Copper (Cu) at (5mm) water depth is shown in figure 4.3. Clearly shows that the temperatures of basinwater for all the stills made with different basin material started equally at 0900hrs but differs after reaching the peak level at 1400hrs, the recorded values for Galvanized Iron, Aluminum and Copper are 53°C, 56°C and 62°C respectively. At 1500hrs the still made with Copper as basin material recorded highest basinwater temperature up till 1600hrs when they all decreases simultaneously. It also shows that during the late

hours of afternoon period (i.e. from 1400hrs to 1600hrs), the basin water temperatures is slightly greater for still with Galvanized Iron (GI) basin material followed by Aluminum (Al) then Copper (Cu) due to it lower thermal conductivity because material with higher thermal conductivity transfer heat faster, leading to quicker cooling (Maqboolet al., 2023). Likewise in the case of morning period when the solar radiation is high, still with Copper (Cu) as basin material shows high basin water temperatures followed by Aluminum (Al) then Galvanized Iron (GI) due to it higher thermal conductivity (Gnanarajet al., 2022).

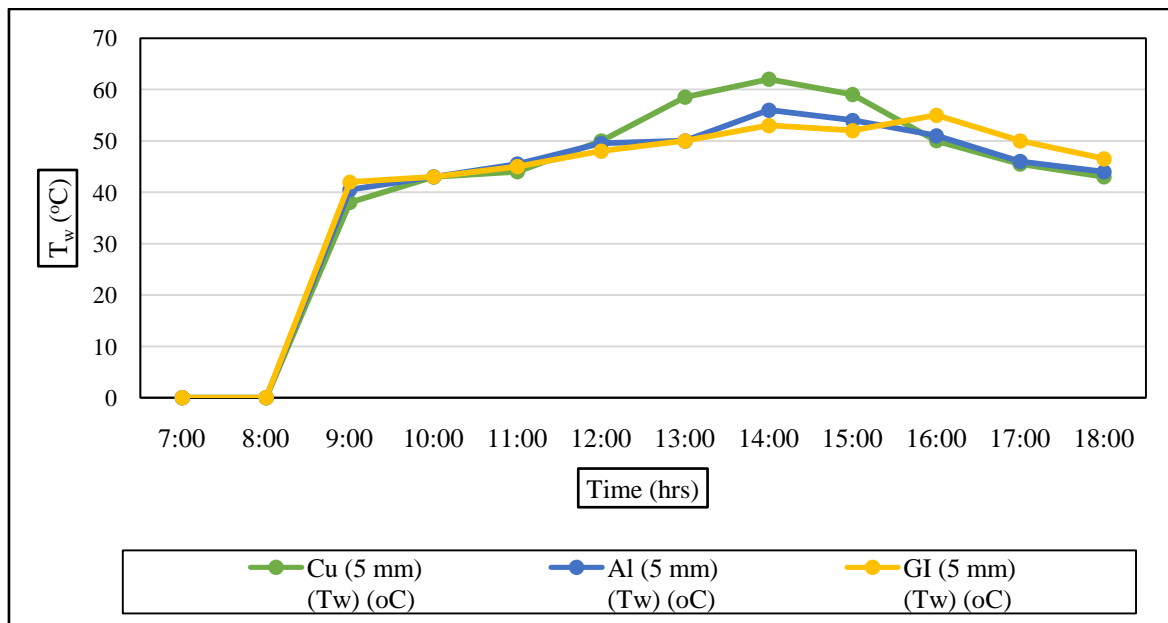


Figure 4.3: Hourly Variation of Basinwater Temperature with Time at (5 mm) Water Depth.

Figure 4.4: Shows cumulative daily distillate yields of stills with different basin materials; Galvanized Iron (GI), Aluminum (Al) and Copper (Cu), it shows clearly from the chart that for the three basin materials we attained the highest daily yield of 2.73 L/day for Copper basin

material followed by 2.61 L/day for Aluminum basin material then 2.56 L/day for Galvanized Iron basin material. This is due to its higher thermal conductivity and lower or thinner water depth result in faster heating and evaporation (Almajaliet al., 2024).

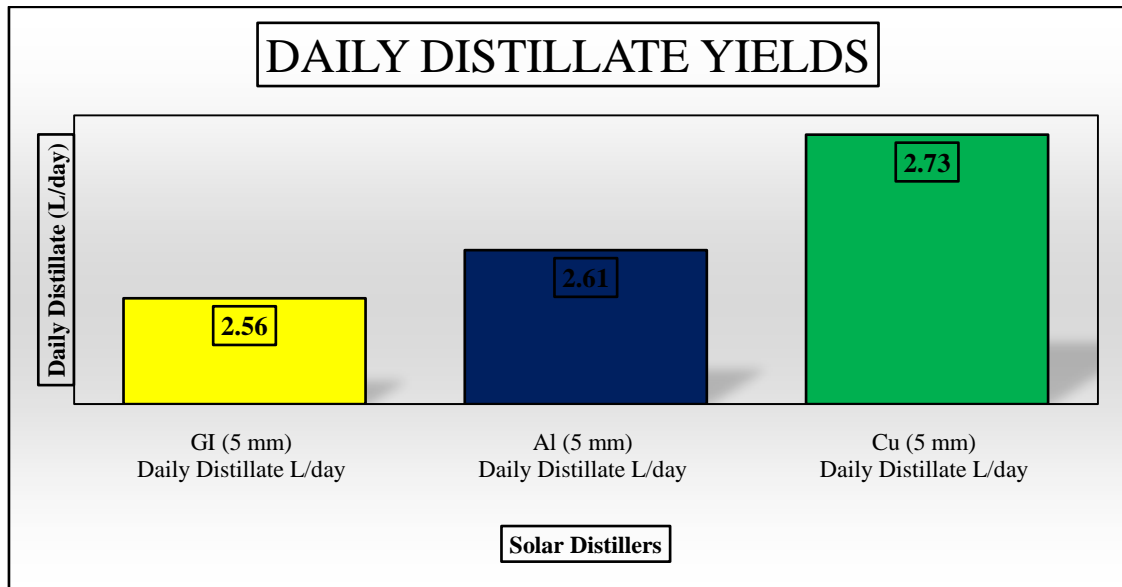


Figure 4.4: Comparison of the Daily Distillate Yields per Different Basin Materials.

The daily efficiency comparison for the three different solar stills with different basin materials, they are Galvanized Iron (GI), Aluminum (Al) and Copper (Cu) at (5mm) respectively is shown in figure 4.5. The chart shows

clearly that distiller with Copper (Cu) as basin material have the highest efficiency followed Aluminum (Al) basin material then Galvanized Iron (GI) basin material.

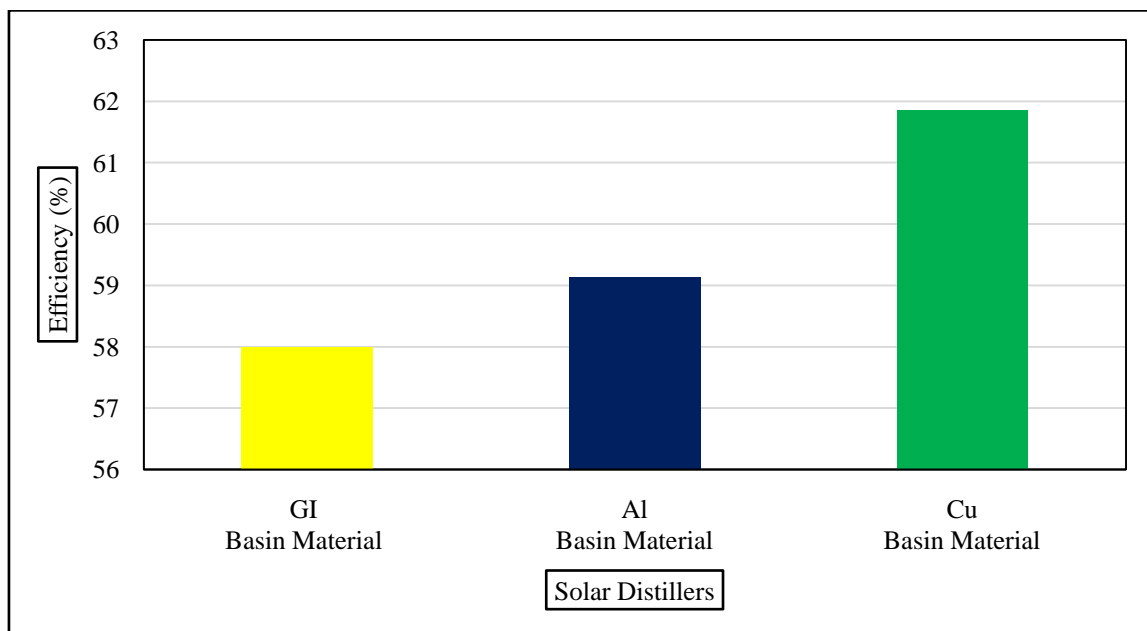


Figure 4.5: Daily Efficiencies Comparison for Three Stills per Different Basin Materials.

VII. CONCLUSION

The major objective of this investigation is to develop a CFD model of single slope single basin solar distillation still and compare the effects of different basin materials (Copper (Cu), Aluminum (Al) and Galvanized Iron (GI) on its performance.

The modelling and simulation has been carried out for three 3-D single slope passive solar stills by specifying different parameters and values by the application of Computational Fluid Dynamics (CFD). The simulation arrangement made as per dimensions explained above. Glasscover

temperature, surface water temperature, basin temperature, ambient temperature, and solar intensity were measured at a regular period of interval initiated at 0700hrs. After initialization of the solution, the results have been obtained in the form of different types of contours and graphs in section 4. From the results obtained, single slope solar still made with Copper (Cu) as basin material achieved highest daily distillate productivity followed by still made with Aluminum (Al) as basin material then Galvanized Iron (GI). Still made with Copper (Cu) as basin material has greater efficiency and daily distillate yield of 61.85% and 2.73 L/day respectively, compared to stills made with Aluminum (Al) and Galvanized Iron (GI) which have daily distillate yields and efficiencies of 2.61 L/day and 59.13% and 2.56 L/day and 57.99% respectively. Also based on the simulation result obtained, it was found that the major parameter which is responsible for the productivity of the distillate water are; water temperature, glass temperature, solar radiation, volume of input water etc.

ACKNOWLEDGEMENTS

The Authors wishes to thank Physics Department and Kebbi State University of Science and Technology, Aliero.

REFERENCES

- [1]. Ahmed, F. E., Khalil, A., & Hilal, N. (2021). Emerging desalination technologies: Current status, challenges and future trends. *Desalination*, **51**(7), 115-183.
- [2]. Ahmed, M. M., Alshammari, F., Abdullah, A. S., & Elashmawy, M. (2021). Basin and tubular solar distillation systems: a review. *Process Safety and Environmental Protection*, **150**(3), 157-178.
- [3]. Alawad, S. M., Mansour, R. B., Al-Sulaiman, F. A., & Rehman, S. (2023). Renewable energy systems for water desalination applications: A comprehensive review. *Energy Conversion and Management*, **28**(6), 117-135.
- [4]. Almajali, T. A. H., Ismail, F. B., Kazem, H. A., Gunnasegaran, P. A., Shurafa, S. M. A., & Al-Muhsen, N. F. (2024). Enhanced water production and improving solar water distillation efficiency of double-slope solar stills: Modeling and validation. *Thermal Science and Engineering Progress*, **53**(4), 102-712.
- [5]. Appiah, R., Zhou, L., Boadi, E. B., Nsiah, T. K., Ayamba, E. C., Minkah, A. Y., & Asante, H. K. (2023). The Causal Link between Anthropogenic Activities, Water Pollution and Health-Related Quality of Life from Residents' Perspective: A Review. *International Journal of Scientific Research in Science and Technology*, **10**(2), 211-226.
- [6]. Ashokkumar, V., Flora, G., Venkatkarthick, R., SenthilKannan, K., Kuppam, C., Stephy, G. M., & Ngamcharussrivichai, C. (2022). Advanced technologies on the sustainable approaches for conversion of organic waste to valuable bioproducts: Emerging circular bioeconomy perspective. *Fuel*, **32**(4), 124-313.
- [7]. Chauhan, V. K., Shukla, S. K., Tirkey, J. V., & Rathore, P. K. S. (2021). A comprehensive review of direct solar desalination techniques and its advancements. *Journal of Cleaner Production*, **28**(4), 124-719.
- [8]. Dubey, A., Singh, S. K., & Tyagi, S. K. (2022). Advances in design and performance of dual slope solar still: a review. *Solar Energy*, **24**(4), 189-217.
- [9]. Elewa, M. M. (2024). Emerging and Conventional Water Desalination Technologies Powered by Renewable Energy and Energy Storage Systems toward Zero Liquid Discharge. *Separations*, **11**(10), 2-91.
- [10]. El-Sebaey, M., Hegazy, A., Ellman, A., & Ghonim, T. (2021). Experimental and CFD study on single slope double basin solar still. *ERJ. Engineering Research Journal*, **44**(1), 21-32.
- [11]. Gnanaraj, S. J. P., & Ramachandran, S. (2022). Identification of operational parameter levels that optimize the production in solar stills with plain, corrugated, and compartmental basin. *Environ Sci Pollut Res*, **29**(5), 7096-7116.
- [12]. Jathar, L. D., Ganesan, S., Shahapurkar, K., Soudagar, M. E. M., Mujtaba, M. A., Anqi, A. E., & Safaei, M. R. (2022). Effect of various factors and diverse approaches to enhance the performance of solar stills: a comprehensive review. *Journal of Thermal Analysis and Calorimetry*, **147**(7), 4491-4522.
- [13]. Khashehchi, M., Thangavel, S., Rahmanivahid, P., Heidari, M., Moazzeni, T., Verma, V., & Kumar, A. (2024). Solar

- desalination techniques: Challenges and opportunities. *Highly Efficient Thermal Renewable Energy Systems*, **6**(3), 305-329.
- [14]. Klewicki, J., Sandberg, R., Knopp, T., Devenport, W., Fritsch, D., Vishwanathan, V., & Eca, L. (2024). On the physical structure, modelling and computation-based prediction of two-dimensional, smooth-wall turbulent boundary layers subjected to stream wise pressure gradients. *Journal of Turbulence*, **25**(10-11), 345-368.
- [15]. Kumar, A. (2024). ANSYS Fluent-CFD analysis of a continuous single-slope single-basin type solar still. *Green Technologies and Sustainability*, **6**(2), 100-105.
- [16]. Kumar, R., Kumar, L., Mirjat, N. H., & Harijan, K. (2024). CFD simulation of modified solar still for effective condensation and evaporation: energy and exergy analysis. *Frontiers in Water*, **6**(4), 143-169.
- [17]. Kumar, S., Wang, X., Strachan, J. P., Yang, Y., & Lu, W. D. (2022). Dynamical memristors for higher-complexity neuromorphic computing. *Nature Reviews Materials*, **7**(7), 575-591.
- [18]. Maka, A. O., & Alabid, J. M. (2022). Solar energy technology and its roles in sustainable development. *Clean Energy*, **6**(3), 476-483.
- [19]. Mishra, B. K., Kumar, P., Saraswat, C., Chakraborty, S., & Gautam, A. (2021). Water security in a changing environment: Concept, challenges and solutions. *Water*, **13**(4), 490.
- [20]. Mishra, R. K. (2023). Fresh water availability and its global challenge. *British Journal of Multidisciplinary and Advanced Studies*, **4**(3), 1-78.
- [21]. Mukhopadhyay, A., Duttagupta, S., & Mukherjee, A. (2022). Emerging organic contaminants in global community drinking water sources and supply: A review of occurrence, processes and remediation. *Journal of Environmental Chemical Engineering*, **10**(3), 107-560.
- [22]. Munteanu, C., Teoibas-Serban, D., Iordache, L., Balaurea, M., & Blendea, C. D. (2021). Water intake meets the Water from inside the human body—physiological, cultural, and health perspectives—Synthetic and Systematic literature review. *Balneo and PRM Research Journal*, **12**(3), 196-209.
- [23]. Sharma, A., Mukhopadhyay, T., Rangappa, S. M., Siengchin, S., & Kushvaha, V. (2022). Advances in computational intelligence of polymer composite materials: machine learning assisted modeling, analysis and design. *Archives of Computational Methods in Engineering*, **29**(5), 3341-3385.
- [24]. Siva Sankaran, N. V., & Sridharan, M. (2022). Experimental research and performance study of double slope single basin solar distillation still using CFD techniques. *International Journal of Ambient Energy*, **43**(1), 3796-3803.
- [25]. Sonawane, C., Alrubaie, A. J., Panchal, H., Chamkha, A. J., Jaber, M. M., Oza, A. D., & Burduhos-Nergis, D. P. (2022). Investigation on the impact of different absorber materials in solar still using CFD simulation—economic and environmental analysis. *Water*, **14**(19), 30-31.
- [26]. Tariq, A., & Mushtaq, A. (2023). Untreated wastewater reasons and causes: a review of most affected areas and cities. *Int. J. Chem. Biochem. Sci*, **23**(1), 121-143.
- [27]. Uncuoglu, E., Citakoglu, H., Latifoglu, L., Bayram, S., Laman, M., Ilkentapar, M., & Oner, A. A. (2022). Comparison of neural network, Gaussian regression, support vector machine, long short-term memory, multi-gene genetic programming, and M5 Trees methods for solving civil engineering problems. *Applied Soft Computing*, **12**(9), 109-623.
- [28]. Zade, F. A., Ghafurian, M. M., Mesgarpour, M., & Niazmand, H. (2023). Predictive machine learning models for optimization of direct solar steam generation. *Journal of Water Process Engineering*, **5**(6), 104-304.
- [29]. Zallio, M., & Clarkson, P. J. (2022). Designing the metaverse: A study on inclusion, diversity, equity, accessibility and safety for digital immersive environments. *Telematics and Informatics*, **7**(5), 101-909.